Supporting information

A flexible and conductive connection introduced by cross-linked CNTs between submicron Si@C particles for better performance LIBs anode

Qiqi Zhou[a, b, c], Junhao Liu[a, b, *], Xuzhong Gong[a, b, c], Zhi Wang[a, b, c, *]

[a] Key Laboratory of Green Process and Engineering, National Engineering Laboratory for Hydrometallurgical Cleaner Production Technology, Institute of Process Engineering, Chinese Academy of Sciences, Beijing 100190, P.R. China

[b] Innovation Academy for Green Manufacture, Chinese Academy of Sciences, Beijing 100190, P.R. China

[c] School of Chemical Engineering, University of Chinese Academy of Sciences, Beijing 100049, P.R. China

* Corresponding author:

Junhao Liu, PhD, Associate Professor

Email: jhliu@ipe.ac.cn

Zhi Wang, PhD, Professor

Email: zwang@ipe.ac.cn

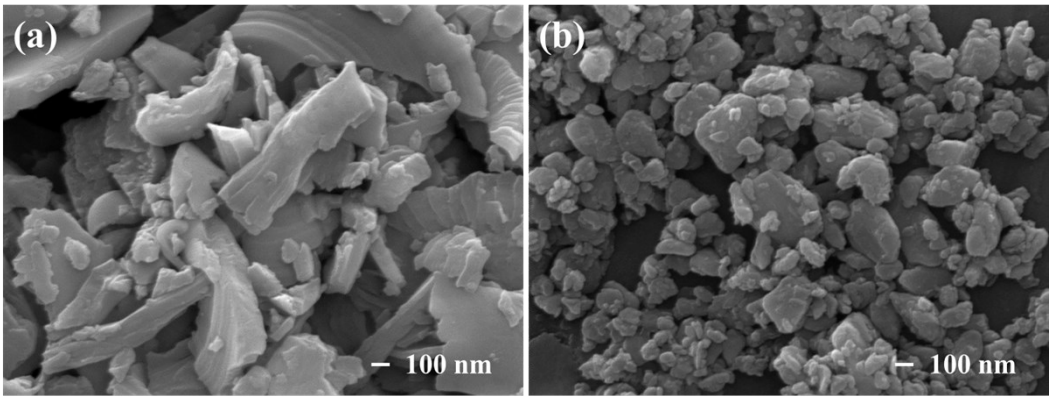

Fig. S1. SEM images of (a) raw materials from wafer silicon slicing process. (b) Silicon materials after post-treatment.

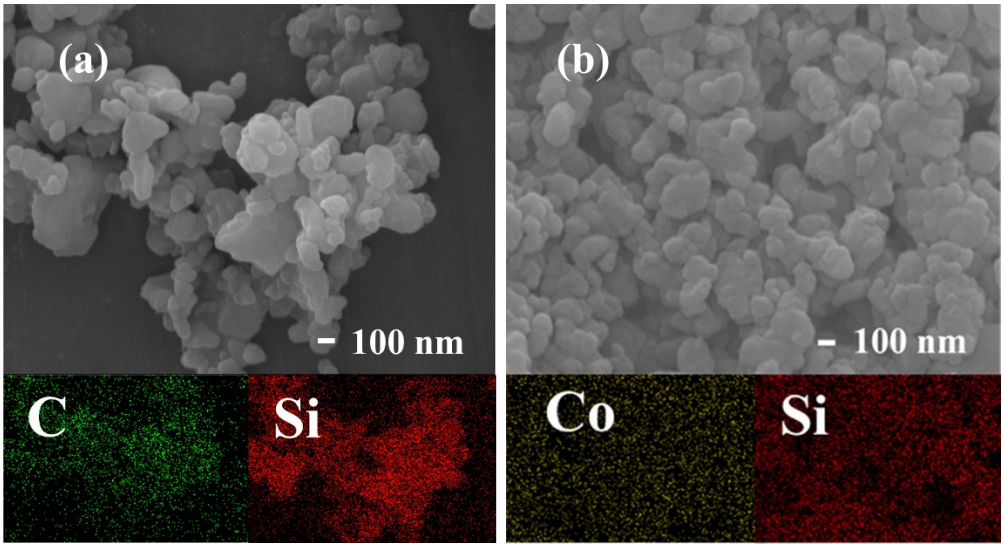

Fig. S2. (a) SEM images of Si@C and (b) Si@C@$Co(OH)_2$.

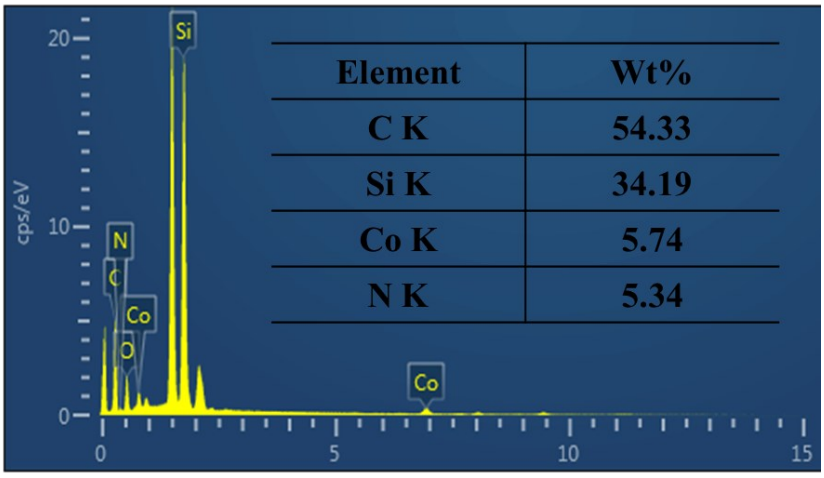

Element	Wt%
C K	54.33
Si K	34.19
Co K	5.74
N K	5.34

Fig. S3. EDX spectrum of Si@C/CNTs.

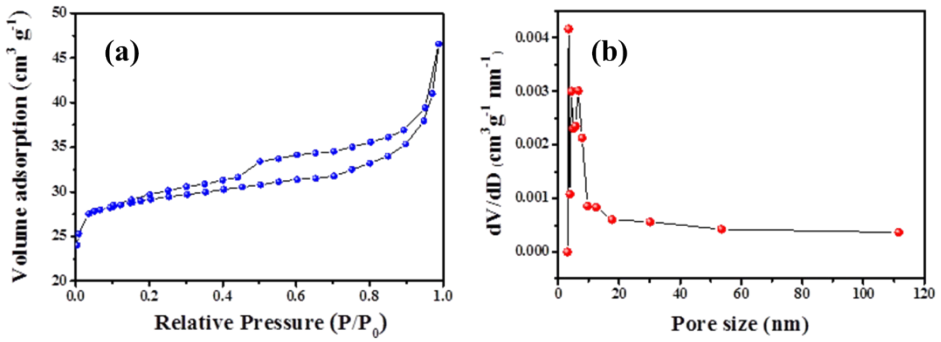

Fig.S4. (a) The nitrogen adsorption/desorption isotherm and (b) the pore size distributions for Si@C/CNTs.

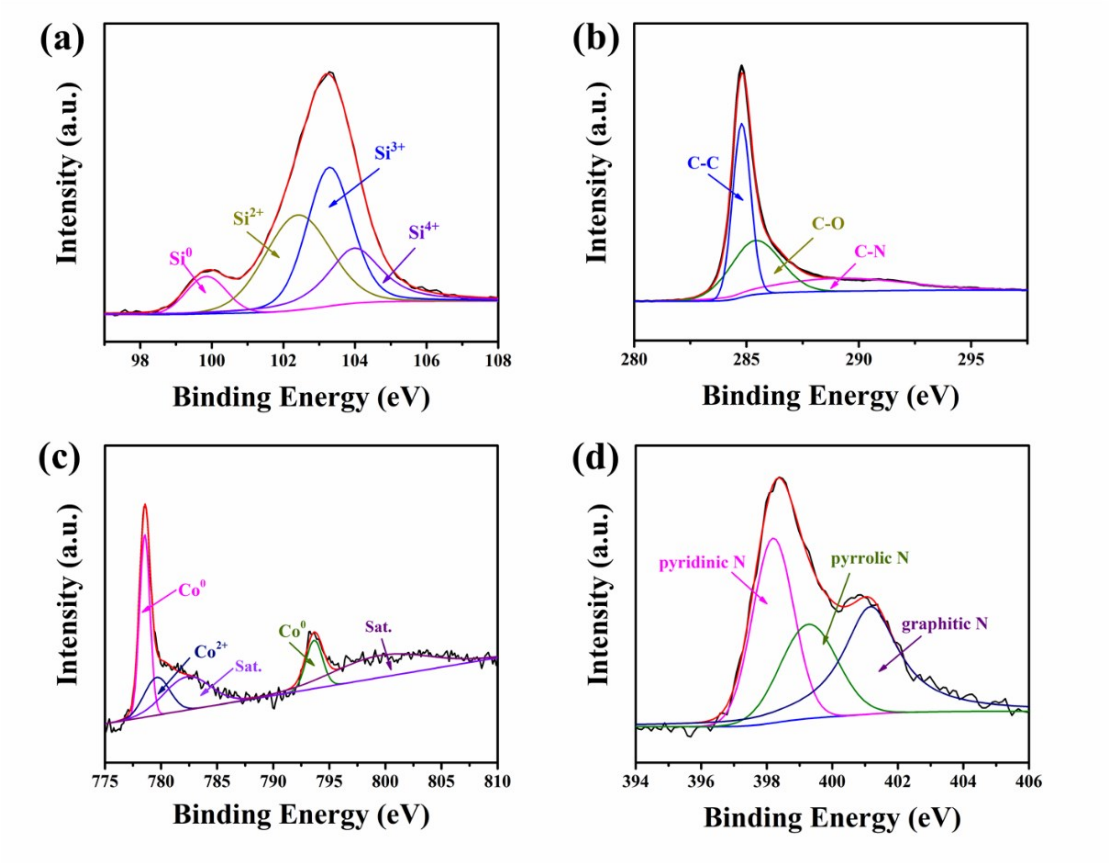

Fig. S5. (a) Si 2p spectrum, (b) C 1s spectrum, (c) Co2p spectrum and (d) N 1s spectrum of Si@C/CNTs.

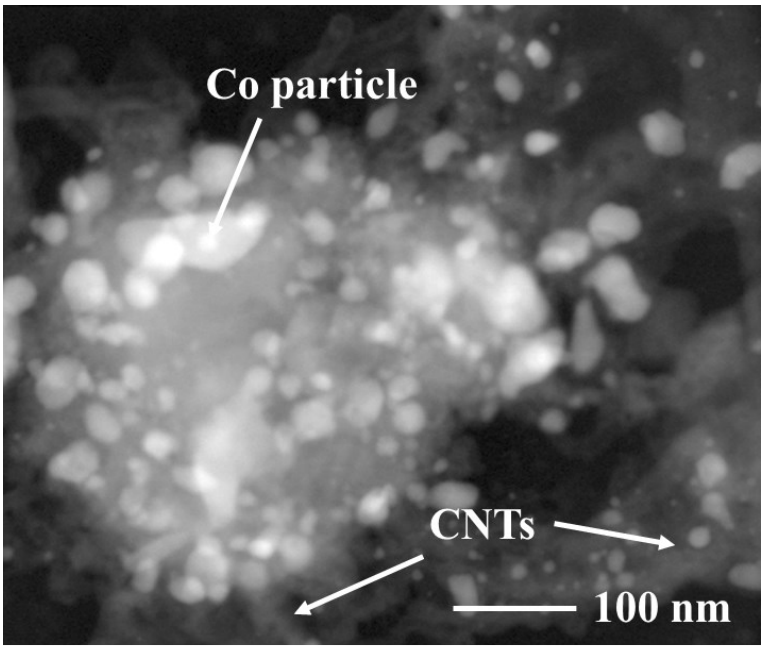

Fig. S6. TEM image of Si@C/CNTs

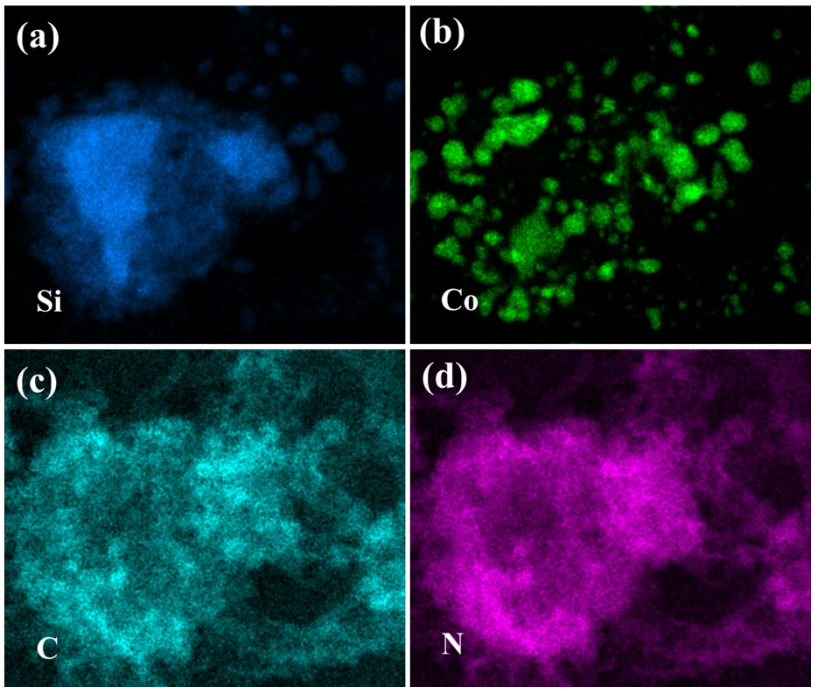

Fig. S7. EDX mapping images for Fig. S6

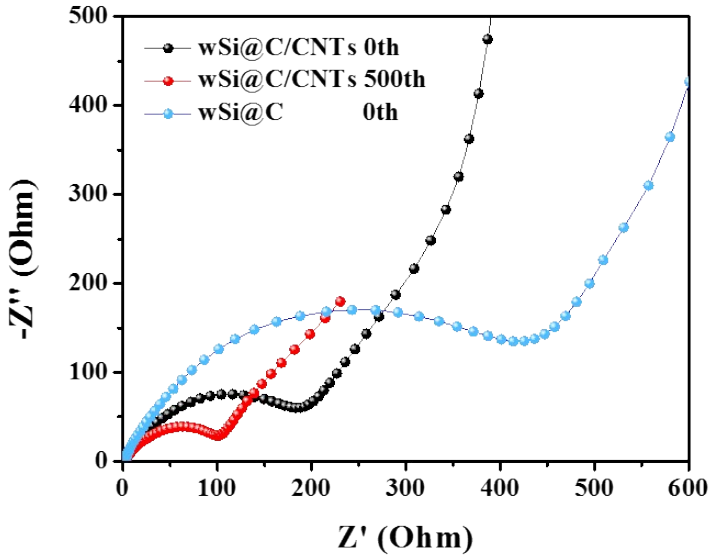

Fig. S8. Nyquist plots of Si@C electrode and Si@C/CNTs electrode in fresh state and Si@C/CNTs electrode after 500 cycles. (e)

Table S1. Percentage of Pyridinic N, Pyrrolic N and Graphitic N of Si@C/CNTs from high-resolution XPS spectra.

	Pyridinic N	Pyrrolic N	Graphitic N
Percentage(% wt)	34.8	24.4	40.8

Table S2. Comparison of the electrochemical performance of photovoltaic waste Si based electrode for lithium-ion batteries.

Sample	Current density ($A\ g^{-1}$)	Cycling stability ($mAh\ g^{-1}$)	Refs.
Si@C/CNTs	0.5	1000.7 (500 cycles)	This work
sm-Si@C/Gr	1.0	1192 (100 cycles)	1
Si@C-G	0.1	401（100 cycles）	2
Si-kerf electrode	C/5	~1000 (300 cycles)	3
Si–Ni anode	0.05	915 (90 cycles)	4
Si-GR composite	0.2	~1050 (50 cycles)	5
Si-MP/Carbon composite	0.5	800 (100 cycles)	6
NanoSi@G	0.45	1138 (150 cycles)	7
C−Si composite	0.3	880 (51 cycles)	8

References

1 B. Lee, T, Liu, S. K. Kim, H. K. Chang, K. Eom, L. X. Xie, S. Chen, H. D. Jang, S. W. Lee, Submicron silicon encapsulated with graphene and carbon as a scalable anode for lithium-ion batteries, Carbon, 2017, 119, 438-445.

2 S. Y. Zhang, J. Xie, C. Y. Wu, X. B. Zhao, A low-cost preparation of Si@C composite anode from Si photovoltaic waste, Inter. J. Electrochem. Sci., 2020, 15, 6582-6595.

3 N. P. Wagne, A. Tron, J. R. Tolchard, G. Nioa, M. P. Bellman, Silicon anodes for lithium-ion batteries produced from recovered kerf powders, J. Power Sources, 2019,414, 486-494.

4 C. J. Chen, T. Mori, A. Jena A, H. Y. Lin, N. H. Yang, N. L. Wu, H. Chang, S. F. Hu, R. S. Liu, Optimizing the Lithium Phosphorus Oxynitride Protective Layer Thickness on Low-Grade Composite Si-Based Anodes for Lithium-Ion Batteries, ChemistrySelect, 2018, 3, 729-735.

5 S. K. Kim, H. Kim, H. Chang, B. G. Cho, J. X. Huang, H. Yoo, H. Kim, H. D. Jang, One-step formation of silicon-graphene composites from silicon sludge waste and graphene oxide via aerosol process for lithium ion batteries, Sci. Rep., 2016, 6, 1-8.

6 H. G. Tan, J. G. Duh, Processing silicon microparticles recycled from wafer waste via Rapid Thermal Process for lithium-ion battery anode

materials, J. Power Sources, 2016,335, 146-154.

7 Q. Bao, Y. H. Huang, C. K. Lan, B. H. Chen, J. G. Duh, Scalable upcycling silicon from waste slicing sludge for high-performance lithium-ion battery anodes, Electrochim. Acta, 2015,173, 82-90.

8 C.Y. Chou, J. R. Kuo, S. C. Yen, Silicon-based composite negative electrode prepared from recycled silicon-slicing slurries and lignin/lignocellulose for Li-ion cells, ACS Sustain. Chem. Eng., 2018, 6, 4759-4766.